Development 134, 3795-3804 (2007) doi:10.1242/dev.02882

Slit and Robo control the development of dendrites in *Drosophila* CNS

Marie-Pierre Furrer, Irina Vasenkova, Daichi Kamiyama*, Yaira Rosado and Akira Chiba*,†

The molecular mechanisms that generate dendrites in the CNS are poorly understood. The diffusible signal molecule Slit and the neuronally expressed receptor Robo mediate growth cone collapse in vivo. However, in cultured neurons, these molecules promote dendritic development. Here we examine the aCC motoneuron, one of the first CNS neurons to generate dendrites in *Drosophila*. Slit displays a dynamic concentration topography that prefigures aCC dendrogenesis. Genetic deletion of Slit leads to complete loss of aCC dendrites. Robo is cell-autonomously required in aCC motoneurons to develop dendrites. Our results demonstrate that Slit and Robo control the development of dendrites in the embryonic CNS.

KEY WORDS: Dendrite, Slit, Robo

INTRODUCTION

Neurons in the CNS develop their dendrites at precise locations and with stereotyped morphology. The typical sequence of neuronal differentiation in vivo is that axogenesis in individual neurons precedes their dendrogenesis (Kim and Chiba, 2004; Westerfield et al., 1986). As a result, when dendrites first appear in the embryonic CNS, axons have already laid out basic fascicle organizations. In many animals, a neuropil, the region enriched with synapses, develops where longitudinal and commissural axon fascicles intersect. Both the molecular heterogeneity among neuronal processes at the neuropil and the fact that each neuron has multiple compartments complicate the dissection of molecular mechanisms that control the development of dendrites in the CNS.

Slit, an evolutionarily conserved signaling molecule, is expressed by midline cells (Rothberg et al., 1988; Rothberg et al., 1990; Yuan et al., 1999; Zou et al., 2000). Slit is a large (190 kDa) secreted protein with four leucine-rich repeats, seven or more EGF (epidermal growth factor) domains, and a cysteine knot (Rothberg et al., 1990). The second leucine-rich repeat is required to bind Robo, a transmembrane receptor expressed by neurons (Howitt et al., 2004). Acting through Robo family receptors (Brose et al., 1999; Li et al., 1999), Slit repels axonal growth cones from the midline during early neural development (Brose et al., 1999; Erskine et al., 2000; Hao et al., 2001; Kidd et al., 1999). However, Slit expression continues through later stages of development (Godenschwege et al., 2002; Johnson et al., 2004). During its emergence, the neuropil is directly contacted by Slit-bearing filopodia from midline cells (Vasenkova et al., 2006), and Slit becomes enriched in the neuropils (Johnson et al., 2004). Study in cultured mammalian cortical and sensory neurons demonstrates that Slit signaling can promote the branching of neurites (Ozdinler and Erzurumlu, 2002; Wang et al., 1999; Ward et al., 2005; Whitford et al., 2002). Similarly, overexpression of Slit causes abnormal axonal branching of Mauthner neurons in zebrafish embryos (Yeo et al., 2001). Correlation between *slit* gene expression and axonal arborization has been noted in vivo, as well (Miyashita et al., 2004; Ozdinler and Erzurumlu, 2002; Ward et al., 2005; Whitford et al., 2002). However, the distribution of Slit protein within the developing CNS has not been described. In particular, whether or not Slit is present prior to the onset of dendrogenesis has not been established. Also, analyses on *slit/slit* mutants have so far focused on early stages of embryogenesis and, therefore, the potential ability of Slit to control dendritic development remains untested in vivo.

The Robo receptor has five extracellular immunoglobulin domains, three extracellular fibronectin type-3 domains, a single transmembrane domain, and several conserved cytoplasmic motifs (Kidd et al., 1998). The first and second immunoglobulin domains are required for binding to Slit (Liu et al., 2004). In addition to growth cone repulsion (Brose et al., 1999; Erskine et al., 2000; Hao et al., 2001; Kidd et al., 1999), Robo has also been implicated in Slit-induced branching and arborization (Miyashita et al., 2004; Ozdinler and Erzurumlu, 2002; Whitford et al., 2002). Whitford et al. (Whitford et al., 2002) overexpressed a cytoplasmically truncated form of Robo in cultured mouse cortical neurons leading to the inhibition of collateral branching of neurites. This result has been interpreted as evidence for endogenous Robo function being required during the development of dendritic and/or axonal arbors. Like its ligand Slit, in vivo Robo expression persists throughout neuronal differentiation. In *Drosophila*, Robo, as well as three other known receptors for Slit (Robo2, Robo3 and Syndecan) are enriched where the neuropil emerges along the longitudinal fascicles and remains abundant there through the end of embryogenesis (Johnson et al., 2004; Rajagopalan et al., 2000; Simpson et al., 2000; Steigemann et al., 2004). Such an expression pattern of Robo in the embryonic CNS is consistent with its proposed role in controlling dendrogenesis. However, genetic analysis of the role of Robo in late-stage embryos is complicated by the fact that this receptor is also required to guide axonal and dendritic growth cones of many neurons at earlier stages of development (Furrer et al., 2003; Kidd et al., 1998; Wolf and Chiba, 2000).

In this study, we examine the role of Slit and Robo in the context of dendritic development through in vivo single-cell analysis. We focus on the aCC (anterior corner cell) motoneuron, one of the first CNS neurons to generate dendrites in *Drosophila* embryos and one that can be visualized and manipulated genetically at the single-cell level (Furrer et al., 2003; Landgraf et al., 1997). We conducted a

Department of Cell and Developmental Biology, University of Illinois, Urbana, IL 61801, USA.

*Present address: Department of Biology, University of Miami, Coral Gables, Florida, USA
†Author for correspondence (e-mail: akira.chiba@miami.edu)

Accepted 4 July 2007

series of experiments using loss-of-function mutant analysis, single-cell genetic rescue and RNAi, quantitative immunocytochemistry and deliberate overexpression. Based on these results, we propose a way in which the diffusible signal molecule Slit and the neuronally expressed receptor Robo control the development of dendrites in the CNS of *Drosophila* embryos.

MATERIALS AND METHODS

Fly stocks

Genotypes and sources of the *Drosophila* stocks used in this study are: $slit^2/slit^2$ (Slit null; Bloomington *Drosophila* Stock Center), $robo^1/robo^1$ (Robo null; C. Goodman, University of California, Berkeley, CA), $robo^4/robo^4$ (Robo null; M. Seeger, Ohio State University, Columbus, OH), Sdc^{10608}/Sdc^{10608} (BDSC), $comm^5/comm^5$ (Commissureless null; M. Seeger), *eve'-GAL4*^{RN2} (GAL4 driver for aCC/pCC and RP2; M. Fujioka and J. Jaynes, Thomas Jefferson University, Philadelphia, PA), *sli'-GAL4*$^{1.0}$ (GAL4 driver for midline glia; C. Klambt, University of Münster, Germany), *GAL4*^{M12} (GAL4 driver for muscle-12; our lab), *UAS-robo*^{WT} (wild-type Robo transgene; C. Goodman), *UAS-robo*^{RNAi} (transgenic 'hairpin' RNAi; P. Garrity, Brandeis University, Waltham, MA) and *UAS-slit*^{WT} (wild-type Slit transgene; R. Jacobs, McMaster University, Hamilton, Canada).

Staging of embryos

Embryos were collected and incubated at 25°C. Developmental stages are indicated in hours at this standard temperature.

Dimensions of embryonic CNS

The mean width of the CNS in the abdominal half-segments 3-5 of unfixed wild-type embryos was 29, 41 and 43 μm at hours 9, 14 and 17, respectively. The mean widths of the CNS in various other genotypes at hour 14 were: 41 μm in $slit^2/+$, 35 μm in $slit^2/slit^2$, 40 μm in Sdc^{10608}/Sdc^{10608}, 39 μm in $robo^4/robo^4$, and 48 μm in $comm^5/comm^5$. Note that all dimensions are calibrated for live whole-mount embryos. Dissection can stretch tissues, and fixation can shrink them by up to 20%. Therefore, we compared dimensions in the CNS both in actual measurements (μm) and in percentages of the main axes, i.e. the medial-lateral axis (from the midline to the edge of the CNS at the mid-point between the centers of the anterior and posterior commissures) and the anteroposterior axis (from one segmental boarder to another). By using the percentages, the measurements from all individual dissected and/or fixed embryos were each calibrated against the live whole-mount embryos of the same age and genotype.

Immunocytochemistry

Antibody raised against a fragment from the EGF repeats (aa1311-1480) of Slit (mAb C555.6D, 1:300 dilution; Developmental Studies Hybridoma Bank) (Rothberg et al., 1990) was used to visualize extracellular Slit protein

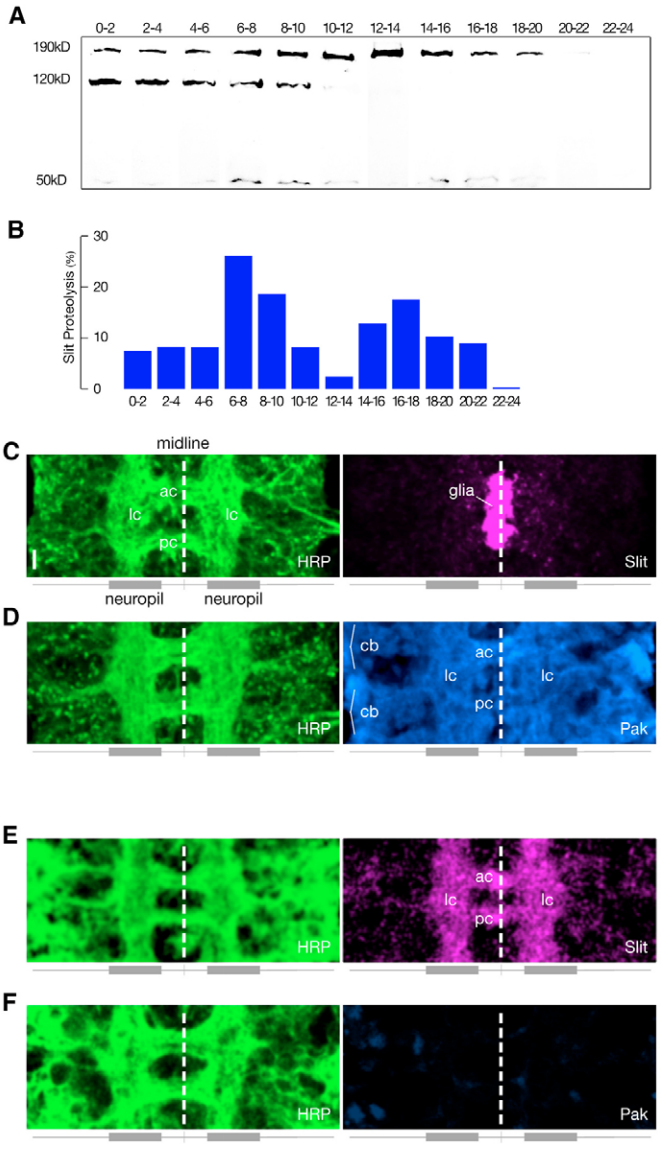

Fig. 1. Slit proteolysis during embryogenesis. (**A**,**B**) Slit proteolysis during embryogenesis. (A) Developmental western blot of whole embryo lysate probed with Slit antibody that recognizes both the full-length and carboxyl-terminus fragment, approximately 190 and 50 kDa, respectively. [Note: a previously unreported band of approximately 120 kDa was detected in tissues from early stages. A similar band was also observed in zygotic $slit^2/slit^2$ null tissues (data not shown). This 120 kDa band is thought to represent either an unknown protein that the Slit antibody recognizes or maternally supplied Slit protein of a previously unreported, truncated form. In the latter case, considering the distance between the Robo-binding domain and the antibody epitope, the protein is unlikely to activate Robo.] (B) Relative concentration of product of Slit proteolysis, i.e. [50 kDa band]/([190 kDa band]+[50 kDa band]). (**C**,**D**) Standard immunocytochemistry of wild-type (+/+) embryonic CNS with Slit (C) and Pak (D) antibodies at hour 14. As in other experiments in this study, the embryos were fillet-dissected and fixed. However, from there on they were subjected to 1 mM Triton X-100 throughout the reminder of the process. Embryos were counter-stained with HRP antibody (green). With detergent treatment, Slit can be detected abundantly in its source, the glia, with additional low-level signals outside the source (C, purple). Anti-HRP recognizes extracellular domains of neuronal cell surface proteins and labels axons in both longitudinal connectives (lc) and commissures (ac and pc; C-D, green). However, the cytoplasmic molecule Pak is detected within the entire CNS, including the longitudinal connectives (lc), commissures (ac and pc) and neuronal cell bodies (cb) (D, blue on right). (**E**,**F**) Detergent-free immunocytochemistry of wild-type (+/+) embryonic CNS with Slit (E) and Pak (F) antibodies at hour 14. Without detergent treatment, Slit is detected mainly along the longitudinal connectives (lc) and commissures (ac and pc) (E, purple on right; also see Fig. 5). This is a very different pattern from the Slit staining using standard immunocytochemistry (compare with C, purple). By contrast, Pak antibody detects very little Pak protein in either axons or neuronal cell bodies (F, blue compare with C, blue). These observations support the idea that the detergent-free method used in this study detects the pool of Slit protein that exists in extracellular space and excludes the pool that is intracellular. Scale bar: 5 μm.

in embryos during hours 9 to 17. This antibody cannot distinguish between the full-length form of the protein and its potential proteolytic in vivo product (Brose et al., 1999). However, developmental western analysis indicated that over 92% of Slit remains full-length during hours 10-14 (Fig. 1A,B). The cell membrane was left untreated (unpermeabilized) with detergent throughout the entire immunological procedure. This excluded from detection the pool of Slit protein that is either within the source cells or internalized into neurons and other non-source cells. A parallel test with antibody against the cytoplasmic molecule Pak (p21-activated kinase) (rabbit IgG, 1:400 dilution; source: Y. Takagi, Fukuoka Dental College, Fukuoka, Japan) confirmed that, without detergent treatment, immunocytochemistry at this stage cannot effectively detect proteins within cells in the embryonic CNS (Fig. 1C-F). To preserve relative immunofluorescent intensities, control and experimental embryos were fillet-dissected in parallel in insect saline and immediately fixed for 10 minutes in freshly prepared 4% paraformaldehyde in phosphate buffer (pH 7.4). This allowed direct comparisons among the embryonic CNSs of different stages and different genetic backgrounds. In all cases, *slit/slit* null embryos were also processed for immunocytochemisrty in the same reaction plate. Their average immunofluorescence intensity was used to define the baseline for quantification of the Slit topography in other genotypes. Preparations were rinsed in phosphate buffer for 30 minutes and blocked in 0.2% BSA (bovine serum albumin) in phosphate buffer (PBSB) with 5% normal goat serum for 4 hours. Primary antibodies were added in PBSB with 1% goat serum and incubated overnight at 4°C. Preparations were then washed in phosphate buffer three times for 15 minutes each and blocked again for 15 minutes in PBSB with 5% normal goat serum. Subsequently, fluorescently (FITC, TRITC or Cy5) labeled secondary antibodies (Jackson Laboratories) were added for 2 hours, after dilution in PBSB with 1% goat serum, rinsed in phosphate buffer for 45 minutes, then in 0.1% Tween 20 in PBS for 15 minutes, and mounted in Prolong medium (Molecular Probes). Addition of Tween 20 at this concentration reduced the background while cellular membranes remained largely intact. FITC-conjugated HRP (horseradish peroxidase) antibody (Jackson Laboratories) was used to determine the position of the neuropil and longitudinal axon fascicles.

Confocal microscopy

Confocal images were collected using a Zeiss LSM510 confocal microscope with 40× 1.3 NA oil-immersion objective lens. The pinhole was set so that an effective optical slice was less than 1.1 μm. *z*-stack optical sections were collected in 0.5 μm steps. Control and experimental embryos were scanned at the same confocal settings and laser power that did not result in oversaturated pixels. The protein distribution along the medial-lateral axis of the CNS was analyzed using IPLab (BD Biosciences, Rockville, MD) and Adobe Photoshop as an averaged single-line profile representing the mean fluorescence intensities of a defined volume within a hemisegment of the CNS as schematically shown in Fig. 2A,B. The final concentration topography of extracellular Slit was compiled using data from multiple hemisegments. Each pixel in the profile represents the mean fluorescent intensity of approximately 10,000 individual pixels from original images.

Single-cell labeling

Individual aCC motoneurons were retrogradely labeled with the lipophilic fluorescent dye DiI as described previously (Furrer et al., 2003). Tracings of these motoneurons were done on projected DiI fluorescent images (Fig. 2C,D for an example).

Size of aCC dendrites

As a measurement of the dendrite size in aCC, the tips of dendritic processes that extended more than 1 μm from the axon shaft were counted, and their positions relative to the midline noted.

RESULTS

Dendrogenesis in the embryonic CNS

To gain insights into the molecular mechanisms that control dendrogenesis in the CNS, we examined the development of the aCC motoneuron. aCCs occur as a bilateral pair in each segment,

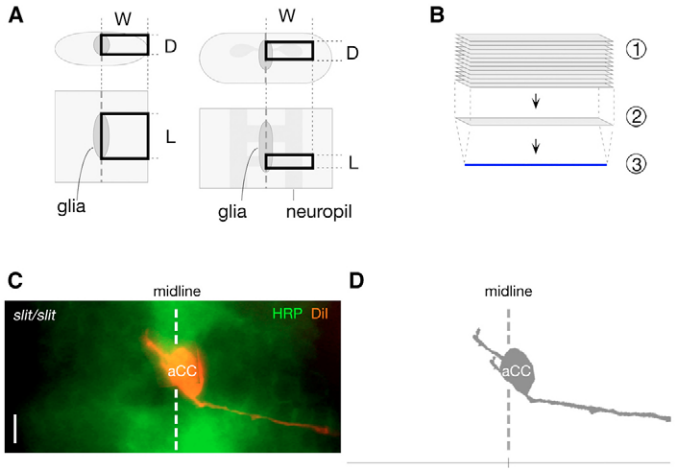

Fig. 2. Quantification of Slit immunocytochemistry and the morphology of aCC. (**A**) Cross-sectional and dorsal views of CNS at early (left) and late (right) stages. The dimensions of the quantified volume (box) are: width (W), 30.0 μm from the midline: depth (D), 5.3±0.4, 5.2±0.2 and 7.7±0.3 μm between the dorsal and ventral sides of the midline glia cluster at hours 9, 14 and 17, respectively; and length (L) 11.3±0.3 μm from the anterior to posterior ends of the midline glia cluster at hour 9, and 4.5±0.2 and 4.7±0.1 μm from the anterior to the posterior ends of the posterior commissure at hours 14 and 17. (**B**) The *z*-stack images (1) are summed into a single 2D image (2) and then consolidated into a single line (3) (see Materials and methods). (**C**,**D**) DiI-labeled aCC (red) in the live wild-type embryo stained with anti-HRP antibody (green, C), from which the tracing of the aCC is obtained (D; see Fig. 7b bottom). Scale bar: 5 μm.

and are among the first neurons to be born and to generate dendrites within the embryonic CNS (Fig. 3A). Dendrogenesis in aCCs can be examined within the CNS of wild-type or mutant embryos through retrograde labeling with fluorescent DiI (Furrer et al., 2003). In addition, an available GAL4 driver (*eve'-GAL4*) (Fujioka et al., 2003) was used to achieve cell-specific expression of various transgenes in aCC. As with other neurons in vivo (Kim and Chiba, 2004), the aCC undergoes a period of axogenesis before initiating dendrogenesis. At hour 9 of wild-type embryogenesis, the aCC produces a single axon that extends laterally toward its target, muscle-1, about 100 μm from the aCC cell body. Beginning at hour 13, about 1 hour before the axonal growth cone of the aCC contacts muscle-1, the aCC begins to develop its main dendrites within the newly emerging neuropil, as collateral processes from the CNS portion of its axon. At the same time, the aCC also extends a medially directed growth cone that subsequently crosses the midline. This second growth cone eventually develops into contralateral dendrites. In this study, we focused on the first dendrites that the aCC develops ipsilaterally. By hour 14, the aCC has extended several filopodia-like dendritic tips along its axon shaft (Fig. 3B,D). By hour 17, the aCC has 15.1±1.5 dendritic tips centered 13.8 μm from the midline (Fig. 3C,E). Such a stereotypy of aCC dendrogenesis allows detection of abnormal development in the CNS of various mutants.

Neuropils, the regions devoid of cell bodies but enriched with synapses, are important landmarks in the CNS. In *Drosophila* embryos, as in many other animals, the neuropils occurs as a bilateral pair in each segment where midline-crossing commissures and longitudinal connectives intersect (Fig. 3A). Starting at hour 9, a neural surface marker, anti-HRP (Jan and Jan, 1982), reveals

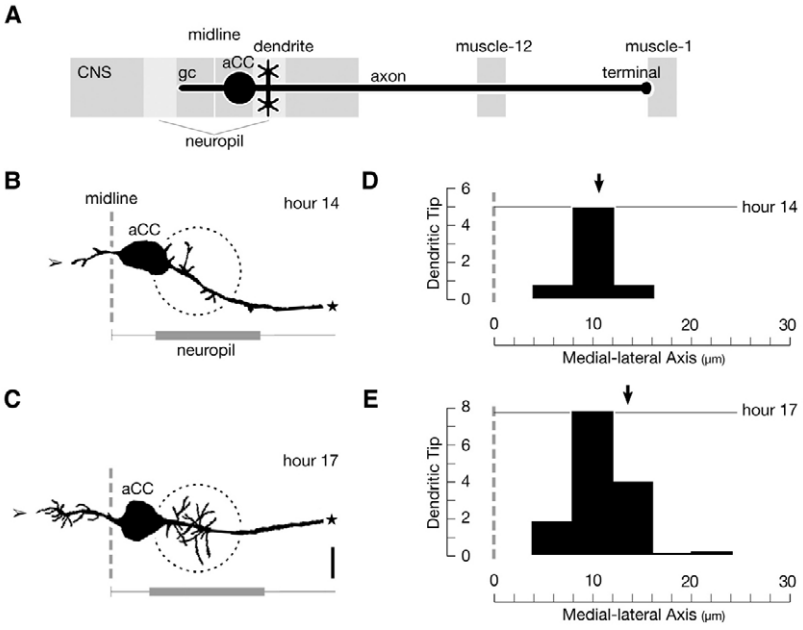

Fig. 3. aCC develops dendrites as collateral processes in the embryonic CNS. (**A**) Schematic of aCC motoneuron in a late-stage embryo. The aCC cell body (aCC) is present near the dorsal midline at each hemisegment in the *Drosophila* embryonic CNS (CNS). The aCC extends a single axon (axon) laterally that cuts across the longitudinal connective, exits the CNS, grows past proximal muscles including muscle-12, then terminates at its target, muscle-1. As its axon approaches the target, aCC begins to develop ipsilateral dendrites (dendrite) as collateral processes from the CNS portion of the axon. A medially directed dendritic growth cone (gc) extends across the midline, which later develops into contralateral dendrites. A neuropil (neuropil) emerges within the longitudinal connective. (**B**,**C**) Tracings of DiI-labeled aCC motoneuron in wild-type embryos at hours 14 (B) and 17 (C). A dotted circle surrounds the main dendrite, and an arrowhead points to the dendritic growth cone that crosses the midline. A star indicates where distal portion of the axon is cropped. Behind the aCC tracing, a shaded region indicates where there is strong anti-HRP staining (see, for example, Fig. 5C left). The width of neuropil is measured as the mean distance between the edges of the HRP-positive longitudinal connective at a point between the centers of anterior and posterior commissures (ac and pc). (**D**,**E**) Histogram of the number of aCC dendritic tips (mean±s.e.m. number per 4 μm) at hours 14 (D, n=6 neurons) and 17 (E, n=14) along the medial-lateral axis. Arrow indicates the mean position. Scale bar: 5 μm.

gradual thickening of this area with neuronal processes. After hour 14, the synaptic vesicle protein Synaptotagmin 1 begins to be detected in the CNS and, by hour 17, it accumulates as puncta through the whole width of longitudinal connectives but not in midline-crossing commissures (data not shown). Nearly concurrently, dendrites of CNS neurons develop within the longitudinal connectives. In our study, we refer to this region from hour 14 onward as the neuropil, and use anti-HRP antibody to estimate its width and position along the medial-lateral axis of the CNS.

Robo is required cell-autonomously

Expression of the *robo* gene in the aCC begins before hour 11 (data not shown). Previous work has shown that in Robo null mutant ($robo^1/robo^1$, $robo^4/robo^4$ or $robo^1/robo^4$) embryos, the aCC develops normally at first, with its axon being guided away from the midline just as in wild-type embryos (Furrer et al., 2003; Wolf and Chiba, 2000). [Note: Wolf and Chiba (Wolf and Chiba, 2000) report one rare incidence in *robo/robo* mutant embryos (out of 38 cases examined) of the aCC abnormally extending its axon across the midline but then following the normal but mirror-image contralateral pathway.] However, the aCC in *robo/robo* embryos exhibits its first visible defects as it begins to develop dendrites. At hour 17, the size of aCC dendrites, measured as the number of dendritic tips, is reduced to 26% of the wild-type size (Fig. 4A). Because aCC development prior to the onset of dendrogenesis is normal in *robo/robo* mutants, it offers a relatively straightforward means for evaluating the role of Robo in dendrogenesis.

To determine whether Robo is required in the aCC during its dendrogenesis, we designed two complementary tests that are bath based on single-cell genetic manipulations. First, we expressed a *robo* RNAi construct (Tayler et al., 2004) transgenically in the aCC in a wild-type background ($eve'\text{-}GAL4^{RN2}/UAS\text{-}robo^{RNAi}$). This cell-specific RNAi against Robo in the aCC reduces its dendritic size to 34% that of wild type. This reduction is similar (P=0.28 by two-tailed t-test) to that observed in the *robo/robo* embryos (Fig. 4C). Second, we transgenically resupplied wild-type Robo protein to the aCC in *robo/robo* embryos ($robo^1/robo^4;eve'\text{-}GAL4^{RN2}/UAS\text{-}robo^{WT}$). Even when surrounded by cells that lack Robo, this cell-specific rescue reverts the dendrogenesis defects to almost wild type (Fig. 4B,C). The sub-100% rescue of the phenotype is not simply due to a low level expression of Robo transgene product in the aCC (see below for a probable

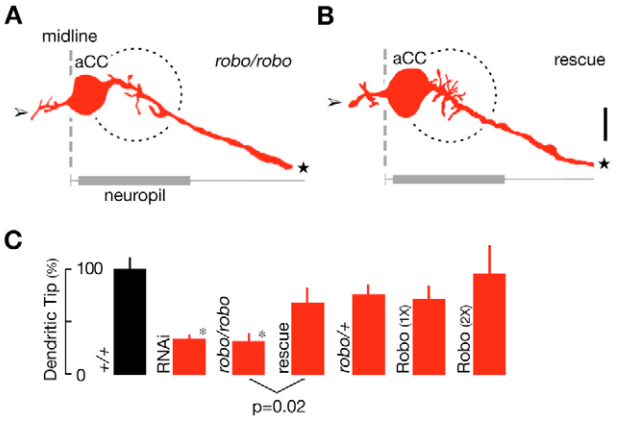

Fig. 4. Robo is required cell-autonomously in the aCC during dendrogenesis. (**A**,**B**) Tracings of $robo^4/robo^4$ (A) and $robo^1/robo^4$ aCCs with cell-specific genetic rescue ($robo^4/robo^1;eve'\text{-}GAL4^{RN2}/UAS\text{-}robo^{WT}$: B) at hour 17. (**C**) Relative sizes of aCC dendrites [measured as mean±s.e.m. number of dendritic tips per neuron, with the wild-type (+/+; value of 15.1) as 100%] in +/+ (n=14), cell-specific RNAi (n=15), $robo^4/robo^4$ and $robo^1/robo^4$ (n=14), rescue (n=7), $robo^4/+$ (n=6), 1× overexpression ($eve'\text{-}GAL4^{RN2}/UAS\text{-}robo^{WT}$; n=11), and 2× overexpression ($eve'\text{-}GAL4^{RN2}/UAS\text{-}robo^{WT},UAS\text{-}robo^{WT}$; n=6). Asterisks indicate P<0.01 by two-tailed t-test against wild type. Scale bar: 5 μm.

explanation). These results indicate that Robo is both necessary and sufficient to cell-autonomously support the dendrogenesis in aCC motoneurons.

Slit topography prefigures dendrogenesis

In the *Drosophila* embryonic CNS, Slit protein is present at neuropils (Johnson et al., 2004). This finding suggests a possible role of Slit during aCC dendrogenesis. However, the time-course for neuropilar accumulation of Slit, a critical parameter for establishing a causal relationship, is unknown. Therefore, we examined the spatiotemporal concentration topography of endogenous Slit, which the emerging axon and dendrites of aCC probably encounter within the embryonic CNS. We used detergent-free immunocytochemistry (see Materials and methods) in order to exclude (a) the pool of Slit protein within the midline glia that is yet to be secreted, and (b) the pool that has been internalized into neurons and non-midline glia and thus is no longer capable of activating Slit receptors on the surface of the aCC and other neurons in the CNS. This leaves only the pool of Slit protein that exists in the extracellular space and, thus, represents the pool capable of signaling various Slit receptors on the neuronal cell surface.

The results reveal a complex concentration topography of Slit within the extracellular space of the CNS that dynamically changes through development (Fig. 5A-D). We quantified Slit in a defined three-dimensional space that roughly matches where the aCC axon extends and its dendrites will develop (Fig. 5, boxed region; also see Fig. 2A,B). We chose three time points: hour 9 before neuropil development, hour 14 immediately after the onset of aCC dendrogenesis, and hour 17, nearly 4 hours after the process has begun. Prior to the emergence of the neuropil, there is a gradient of Slit that descends steeply from its midline source (Fig. 5E). This is when the growth cones of many axons orient themselves, each toward a specific direction with respect to the midline (Furrer et al., 2003; Kidd et al., 1999; Wolf and Chiba, 2000). At this time, the distribution of Slit is similar to many other diffusible signal molecules, as a descending gradient from its source. However, once the neuropil begins to develop, a notable deviation occurs at approximately 10 μm from the midline, where the longitudinal fascicles begin to thicken. Slit starts to accumulate at this position. By hour 14, this local accumulation reaches 43% of the midline level (Fig. 5F). Subsequently, Slit levels at both the midline and neuropils rise continuously. Neuropils begin to emerge at the site of this secondary Slit accumulation. The aCC dendrites also develop at the very site of the Slit enrichment and immediately after, but not before nor long after, local Slit concentration begins to rise there. This spatiotemporal coincidence raises the possibility that Slit at the neuropil is either an inducer or facilitator of dendrogenesis in the aCC.

In the *robo/robo* mutant embryos, the overall amount of Slit protein at hour 14 is reduced to 79% of wild-type amounts (Fig. 6A,B), presumably reflecting the normal Robo function of capturing the protein on the cell surface and its contribution to the establishment of Slit topography. In addition, the secondary accumulation of Slit is medially shifted in the *robo/robo* embryos. This medial shift occurs in an exact parallel to that of the neuropil. aCC dendrites in the *robo/robo* embryos are also medially shifted, and are small when compared with wild-type dendrites (Fig. 4B). The shift in dendritic position matches those of both the neuropil and the local accumulation of Slit (Fig. 6C). As shown above, resupply of wild-type Robo to the aCC results in an increase in the dendritic

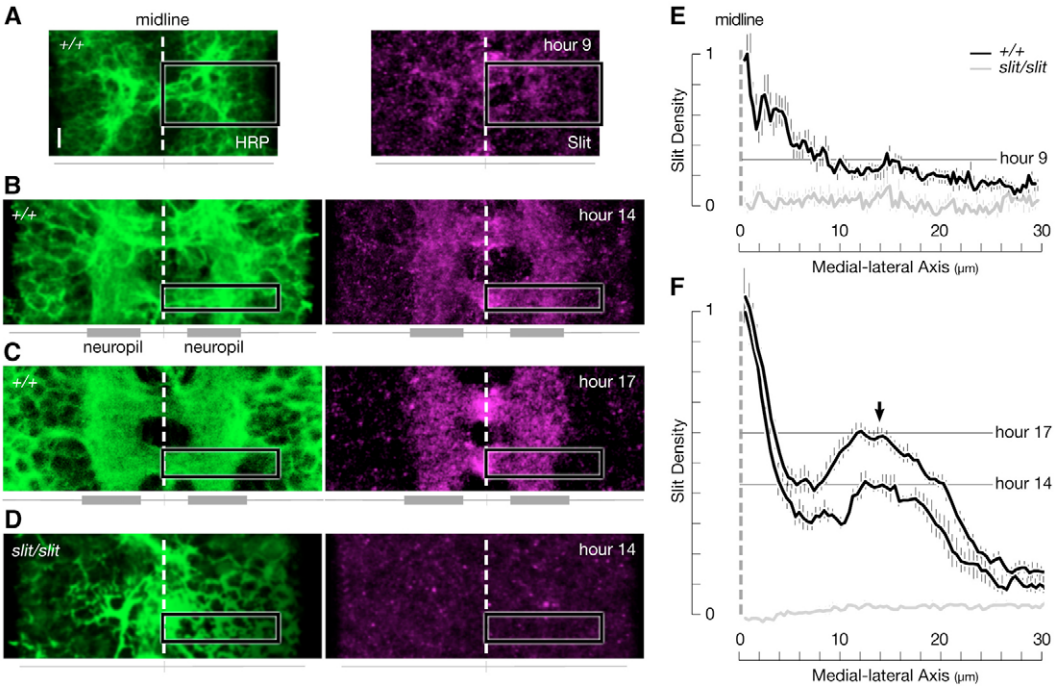

Fig. 5. Slit topography spatiotemporally prefigures dendrogenesis. (**A-D**) Detergent-free immunocytochemistry with anti-HRP, which labels neuronal surface (green), and anti-Slit (purple) in wild-type (+/+) at hours 9 (A), 14 (B) and 17 (C), and in Slit null (*slit*^{2}/*slit*^{2}) embryos at hour 14 (D). Single segments are shown as projected images. The width of CNS is shown by the horizontal line beneath with gray bars indicating the width and position of bilateral neuropils. Boxes outline the region in which Slit density was quantified. (**E**,**F**) Slit concentration topography along the medial-lateral axis (mean±s.e.m.) at hour 9 (*n*=13 half-segments; E), and at hours 14 and 17 (*n*=15 and 13; F). The *slit/slit* tissues (*n*=13 and 14 for hours 9 and 14, respectively) provide the baselines. Slit densities are normalized to the midline level in the wild type at hour 9 (E) or 14 (F). The horizontal lines shows the peak of neuropilar Slit accumulation, and arrows indicate its center. Scale bar: 5 μm.

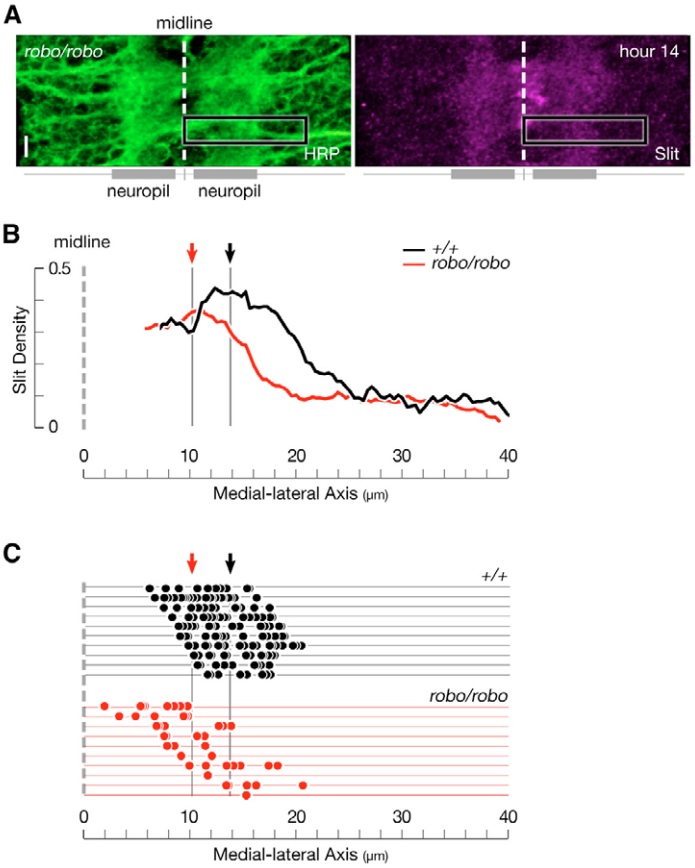

Fig. 6. Slit topography correlates to aCC dendrogenesis in *robo/robo* mutant. (**A**) Detergent-free immunocytochemistry with anti-HRP (green) and anti-Slit (purple) in *robo*^{4}/*robo*^{4} embryos at hour 14. (**B**) Slit concentration topography (neuropilar portion, normalized to the midline level in +/+ at hour 14; see Fig. 3F) in wild type (+/+) (*n*=12) and *robo*^{4}/*robo*^{4} (*n*=12) embryos at hour 14. Arrows indicate the center of the neuropilar concentration. (**C**) Scattergraphs (up to 10 aCCs per genotype) of dendritic tips in +/+ (*n*=14) and *robo*^{4}/*robo*^{4} (*n*=14) at hour 17. Each horizontal line indicates an individual aCC neurons and circles indicate the positions of dendritic tips along its axons. Scale bar: 5 μm.

size, to 70% of wild type (Fig. 4B,C). This reduction in dendritic size in the mutant parallels that of the volume of the local Slit peak (compare Fig. 6B with Fig. 6C). These results suggest that although Robo serves as a receptor detecting the presence of Slit, the amount of Slit at the neuropil modulates Robo activities.

Loss of Slit leads to loss of dendrites

We used genetics to test a potential dendrogenic role of Slit. Unlike vertebrate genomes, the *Drosophila* genome contains only a single *slit* gene (Rothberg et al., 1988). Furthermore, *slit/slit* embryos survive until late embryonic stages, thus providing an opportunity to test the idea that Slit may play a role in dendrogenesis in the CNS. In Slit loss-of-function (*slit*^{2}/*slit*^{2}) mutants, the aCC extends its axon into the periphery (data not shown). Also, it produces a dendritic growth cone that crosses the midline (Fig. 7B, arrowhead). However, the aCC fails to develop any collateral dendrites along its axon (Fig. 7B,C). Motoneurons RP2 and U, too, generate a reduced number of dendrites (data not shown). These results show that loss of Slit leads to a loss of dendrites in the developing CNS.

Potential role of Slit at neuropil

Although dramatic, the loss of aCC dendrites in *slit/slit* embryos (Fig. 7) might not indicate a direct dendrogenic role for Slit. Even before the normal onset of aCC dendrogenesis the CNS midline collapses in these mutant embryos (Kidd et al., 1999; Rothberg et al., 1990; Sonnenfeld and Jacobs, 1994). At the time dendrogenesis would normally occur, the CNS lacks a neuropil (Fig. 5D). It is possible that the emerging neuropil provides factors other than Slit that are responsible for inducing dendrogenesis in the aCC. Alternatively, Slit and the neuropil-derived factor(s) might both be required. To evaluate these possibilities, we examined dendrogenesis in additional genetic backgrounds.

The Commissureless loss-of-function mutation (*comm*^{5}/*comm*^{5}) shifts the neuropil laterally (Fig. 8A left). We reasoned that if the neuropil moves laterally, then the position of the dendrites would probably move laterally, as well. We found that aCC dendrites indeed form at the neuropil, their size being 56% that of wild-type neuropils (Fig. 8B,D). However, to our surprise, Slit is also found at 64% of the wild-type level in the laterally shifted neuropil (Fig. 8A right, also Fig. 8C). Thus, there is a three-way correlation among the neuropil, Slit and aCC dendrites in these embryos.

We next examined Slit heterozygous (*slit*^{2}/+) embryos. With half the dose of the *slit* gene, embryos express Slit protein at 49% of the wild-type level, but otherwise keep the overall Slit topography with accumulation at the midline and the neuropil (Fig. 9A right, also Fig. 9E). Despite that, the animals are viable as heterozygotes, and their CNS and neuropil appears virtually wild type (Fig. 9A left). We reasoned that if the neuropil without a normal amount of Slit were sufficient, then the aCC would still develop normal dendrites at the neuropil. However, we found that the number of aCC dendritic tips in the *slit*/+ embryos dropped to 52% of the wild-type value (Fig. 9C,F).

Syndecan is another cell surface receptor known to bind Slit (Johnson et al., 2004; Steigemann et al., 2004). In *Syndecan* (*Sdc*^{10608}/*Sdc*^{10608}) mutant embryos, we noted a 51% loss of Slit from the neuropil as well (Fig. 9B right, also Fig. 9E). Nevertheless, the neuropil, is relatively normal in size and position (Fig. 9B left). aCC dendrites in the *Sdc/Sdc* embryos develop within the neuropil (Fig. 9D). However, as in the *slit*/+ embryos, the number of aCC dendritic tips drops to 68% of wild-type numbers (Fig. 9D,F). Again, this drop corresponds fairly well to the reduction in the Slit concentration at the neuropil. Thus, in both *slit*/+ and *Sdc/Sdc* embryos, the neuropil remains more or less wild type, while the size of aCC dendrites decreases in parallel to the amount of Slit present at the neuropil.

Sdc/Sdc mutants also provide additional insights. *Sdc/Sdc* and *robo/robo* mutations reduce the size of aCC dendrites similarly, i.e. by 68% and 74%, respectively. However, whereas *robo/robo* embryos lose only 26% of neuropilar Slit, *Sdc/Sdc* embryos lose 60%. These observations are consistent with the idea that Syndecan serves as a co-receptor, that presents Slit to other Slit receptors expressed at the neuropil, whereas Robo functions as a receptor mediating the dendrogenic role of Slit.

These results lead to two conclusions. First, although contributions of yet-to-be-identified neuropil-derived factors cannot be ruled out, both the timing and the relative extent of dendrogenesis are positively correlated to the dynamic presence of Slit at the neuropil. Second, while different receptors, including Robo and Syndecan, can trap Slit protein on the cell surface, it is Robo that is likely to play a major role in signaling with localized Slit during dendrogenesis.

Slit alone is sufficient to induce dendrogenesis

Would presentation of Slit alone be sufficient to induce dendrogenesis? To answer the question, we expressed full-length wild-type Slit in muscle-12, outside the CNS, using a muscle-12-

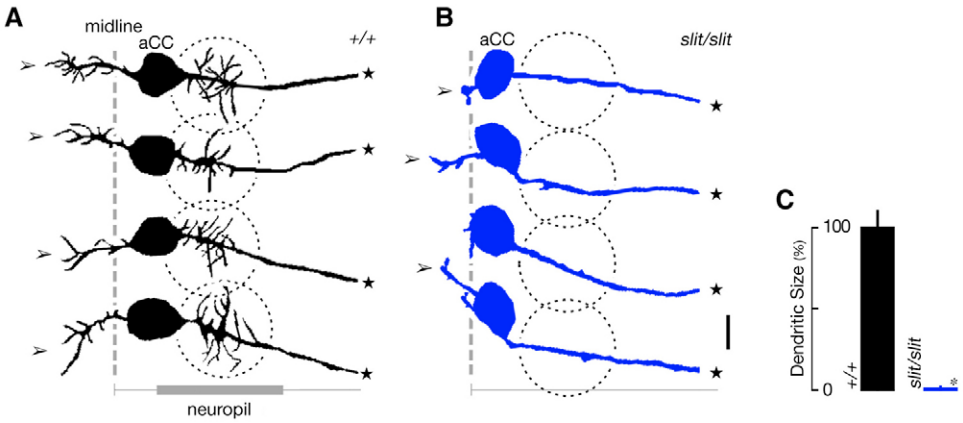

Fig. 7. Loss of Slit leads to loss of aCC dendrites in *slit/slit* mutant. (**A**,**B**) Tracings of wild-type (+/+; A) and *slit*^{2}/*slit*^{2} (B) aCCs at hour 17. (**C**) Relative sizes of +/+ (*n*=14) and *slit*^{2}/*slit*^{2} (*n*=9) aCC dendrites at hour 17. Scale bar: 5 μm.

specific GAL4 driver (*GAL4*^{M12}/*UAS-slit*^{WT}) (see Fig. 3A). The aCC and other ISN (intersegmental nerve) motoneuron axons normally extend beyond muscle-12, before this GAL4 driver starts transgene expression. Normally, these axons are in contact with muscle-12, but do not generate any collateral processes here. Overexpression of Slit in muscle-12 fails to induce any collateral processes (0%, *n*=29 neurons) from any of these axons (Fig. 10A,B circle). By contrast, the ectopic Slit stalls the growth cone of the RP5 motoneuron from its target muscle-12 (100%, *n*=27 neurons) (Fig. 10B arrow). These results give further support to the idea that presentation of Slit alone is not sufficient to induce collateral dendrogenesis from the aCC along its axon.

DISCUSSION

Previous studies have suggested that Slit and Robo promote collateral neurite formation in cultured neurons (Ozdinler and Erzurumlu, 2002; Wang et al., 1999; Ward et al., 2005; Whitford et al., 2002). Our goal in this study was to examine the role of Slit and Robo in the context of in vivo dendrogenesis in the CNS. Dendrogenesis is a late-stage event in the differentiation of neurons. Thus, to uncover the specific role of molecules responsible for dendrogenesis, one must not only demonstrate their loss-of-function phenotype but also isolate their cell-autonomous operation. Furthermore, it is also necessary to uncouple the earlier contribution of the molecules, to either neurogenesis or axogenesis, from their direct contribution during dendrogenesis. We chose to focus on the aCC motoneuron, one of the first CNS neurons to generate dendrites in *Drosophila* embryos and also one that can be genetically manipulated and visualized at the single-cell level. Our results support the conclusion that in neurons Slit, signaling through Robo, is responsible for controlling the timing, positioning, and size of dendrites in the embryonic CNS. They also offer insights into the complexity that surrounds the development of dendrites in vivo.

Single-cell analysis on the role of Robo

In *robo/robo* embryos, the aCC produces small dendrites (Fig. 4B). It is possible that this residual dendrogenesis reflects partial functional redundancy among Robo family receptors. RNAi against the *robo* gene in the aCC also results in small dendrites (Fig. 4C). Conversely, cell-specific resupply of wild-type Robo in the aCC reinstates its ability to grow dendrites (Fig. 4C). These results, together with the fact that the aCC neurons in *robo/robo* embryos have no other defects prior to the onset of dendrogenesis, support the specific role of Robo in dendritic development.

The dendrogenic role of Robo was first demonstrated by Ghosh's group (Whitford et al., 2002). Their key experiment was inhibition of neurite branching in cultured neurons through overexpression of the cytoplasmically truncated Robo. In our hands, similar attempts to use a *Drosophila* version of cytoplasmically truncated Robo have failed to induce any extra or abnormal dendrogenesis in vivo (data not shown). Instead, we show that both genetic deletion and RNAi against the *robo* gene cause dendrogenesis defects in uniquely identified CNS neurons (Fig. 4). The difference in effectiveness of dominant-negative proteins between the mammalian and *Drosophila* neurons might simply reflect whether or not Robo is a rate-limiting factor in a given neuron. Alternatively, data from both Ghosh's group and ours are consistent with Robo being required cell-autonomously during dendrogenesis.

Robo is expressed throughout neuronal development, not just during the period of axon guidance analyzed by the majority of in vivo studies to date. Previously, single-cell analyses in the embryonic *Drosophila* CNS have shown a role for Robo in directing growth cones away from the Slit-secreting midline. Without Robo, the axons of RP2 motoneurons are misguided medially (Wolf and Chiba, 2000). Later, the same Robo-lacking RP2 neurons also misguide their dendritic growth cones towards the midline (Furrer et al., 2003). In comparison to RP2, aCC motoneurons do not normally rely on Robo to properly orient axonal and dendritic growth cones. However, when Robo is overexpressed in the aCC, its dendritic growth cone can be made to avoid the midline (data not shown). In all these cases, it would appear that Robo causes growth cone collapse upon detecting Slit at the midline. By contrast, our study supports a role for Robo in promoting the formation of collateral dendritic processes. aCC motoneurons cell-autonomously require Robo during dendrogenesis (Fig. 4). Clearly, the same receptor has distinct roles, either collapsing growth cones or promoting collateral dendrogenesis, i.e. two seemingly opposite types of cellular responses, sometimes even within a single neuron. Although we do not yet know the underlying mechanism, it is intriguing that migrating myoblasts also exhibit a developmentally regulated response switch of Slit-Robo signaling from repulsion to attraction in *Drosophila* embryos (Kramer et al., 2001).

Insights from Slit topography

The Slit concentration topography of the embryonic CNS exhibits a dynamic four-dimensionality (Fig. 5E,F). Previously, it was postulated that there is a descending gradient of Slit from its source (Goodhill, 2003; Rajagopalan et al., 2000; Simpson et al., 2000).

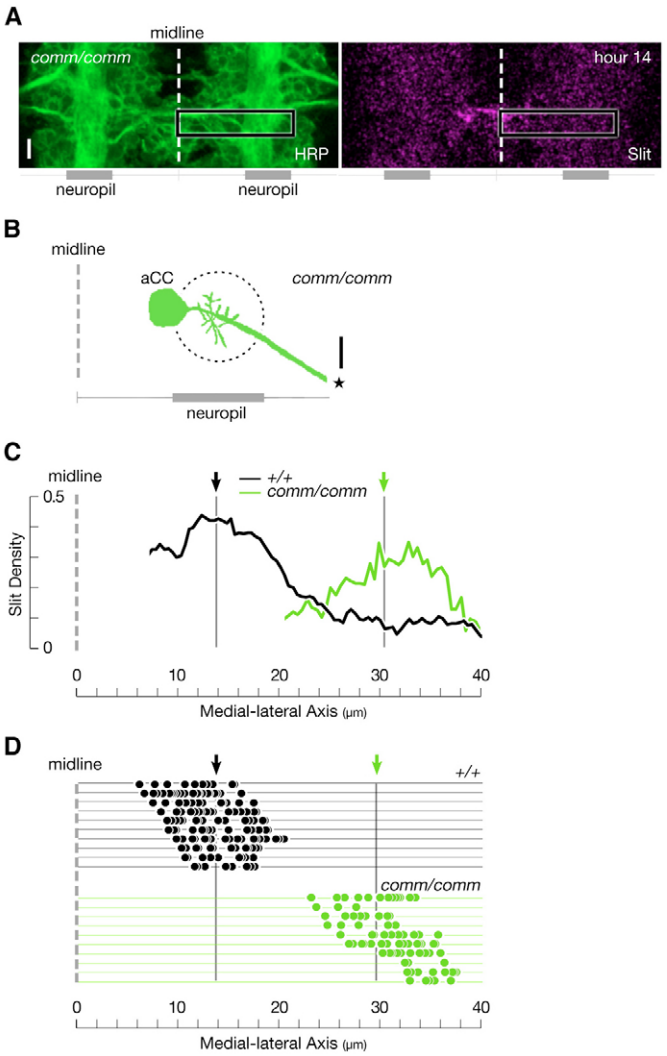

Fig. 8. In *comm/comm* mutants neuropils and aCC dendrites shift laterally in parallel. (**A**) Detergent-free immunocytochemistry with anti-HRP (green) and anti-Slit (purple) in $comm^5/comm^5$ embryos at hour 14. (**B**) $comm^5/comm^5$ aCC at hour 17. (**C**) Slit concentration topography in wild-type (+/+; *n*=4) and $comm^5/comm^5$ (*n*=9) embryos at hour 14. (**D**) Scattergraphs (10 aCCs per genotype) of dendritic tips in +/+ and $comm^5/comm^5$ embryos at hour 17. Scale bar: 5 μm.

Indeed, both in culture media and within imaginal discs, diffusible signaling molecules set up gradients that descend from their source (Tabata, 2001; Tessier-Lavigne et al., 1988). We find that the actual Slit topography in the embryonic CNS is much more complex (Fig. 5). Unlike culture media, the embryonic CNS redistributes molecules such as Netrin (Brankatschk and Dickson, 2006; Hiramoto et al., 2000) and Slit (this study) from their original source. Already by hour 14, the time when the first dendrites begin to form, a prominent secondary accumulation of Slit is present locally 10-20 μm away from the midline source of Slit (Fig. 5F arrow). The local concentration is approximately 43% of that at the midline, and the amount of Slit that is found beyond 10 μm from the midline, the local minimum, is 56% of the total extracellular Slit in the whole CNS.

How does Slit reach the neuropil in such abundance? Slit could accumulate there either through diffusion (Johnson et al., 2004) or direct filopodia-mediated delivery (Vasenkova et al., 2006). Once there, Syndecan plays a role in capturing the extracellular Slit (Johnson et al., 2004) (this study). Our study suggests that the presence of Robo at the neuropil also contributes to Slit capture on cell surface (Fig. 6B). In addition to Syndecan and Robo, at least two more Slit receptors, Robo2 and Robo3, are known in *Drosophila*. When bound to such receptors on the surface of migrating axons, Slit could be transported along commissural and longitudinal fascicles. Individual Robo receptors are expressed in overlapping but distinct sets of neurons (Rajagopalan et al., 2000; Simpson et al., 2000). Plenty of molecular heterogeneity and cellular dynamics exists within the developing nervous system that could contribute to an extensive redistribution of Slit within the CNS.

We propose that neural development utilizes the complex Slit topography to control dendrogenesis. First, the position of the aCC collateral dendrogenesis coincides with the local Still accumulation. Except for the *slit/slit* embryos where there is no Slit present, all other genetic backgrounds examined in our study have aCC dendrites developing where Slit accumulates locally. Second, there is a positive correlation between the size of aCC dendrites and the amount of Slit present. A notable exception is the *robo/robo* embryos, in which the size of aCC dendrites is attenuated due to the loss of Robo, a Slit receptor, in the neuron (Fig. 4). In *Drosophila* embryos, evidence for Slit proteolysis has been presented by Brose et al. (Brose et al., 1999). Because the Slit antibody recognizes the carboxyl terminus region of the protein, it does not distinguish between full-length Slit, which is capable of activating Robo, and the carboxyl-terminus fragment of the proteolytic product, which is not. We have assessed the developmental control over Slit proteolysis. Our quantification shows that, at hour 14, the proteolysis affects only about 8% of the total volume of Slit (Fig. 1B). Independent data also suggest that Slit at the neuropil and beyond is indeed in the form that is capable of stimulating Robo (I.V., M.-P.F. and A.C., unpublished). In our study, we assume that a majority of Slit protein detected by the antibody in the neuropil is in the full-length form, and take the positive correlation between the Slit profile and aCC dendrogenesis to suggest that Slit acts in an instructive role, setting the size of dendrites. Third, the time at which Slit begins to accumulate at the emerging neuropil immediately precedes the initiation of collateral dendrogenesis in the aCC. This indicates that Slit accumulation is not simply a consequence of dendritic development. Instead, the tight spatiotemporal correlation between Slit topography and aCC dendrogenesis supports a model in which Slit plays a crucial role.

The phenotype of *slit/slit* embryos

The *slit/slit* phenotype during the period of dendrogenesis is dramatic. Visualization with the anti-HRP antibody and retrograde DiI labeling in late-stage *slit/slit* embryos reveals that many motoneurons extend out axons in the CNS without Slit. Yet, they fail to initiate dendrites. Thus, the phenotype that motoneurons such as aCCs (Fig. 7B) and RP2s (data not shown) exhibit is unique. However, there is a problem in attributing a direct cause of the dendrite-less motoneurons to the absence of Slit. This is because *slit/slit* embryos form very few axon fascicles, resulting in a virtually neuropil-less CNS (Fig. 5D). Therefore, the dendrogenesis defects observed in *slit/slit* embryos could be accounted for by any of the following three scenarios: (1) the neuropil, not Slit, induces dendrogenesis, (2) Slit alone is required, or (3) both the neuropil and Slit are required. Of these, the third scenario is the most likely (see below).

In vivo complexity that impacts dendrogenesis

Hints about the additional factors that impact dendrogenesis are available not only where neurons develop dendrites, but also where they do not. Except for *slit/slit*, all other genotypes examined in our

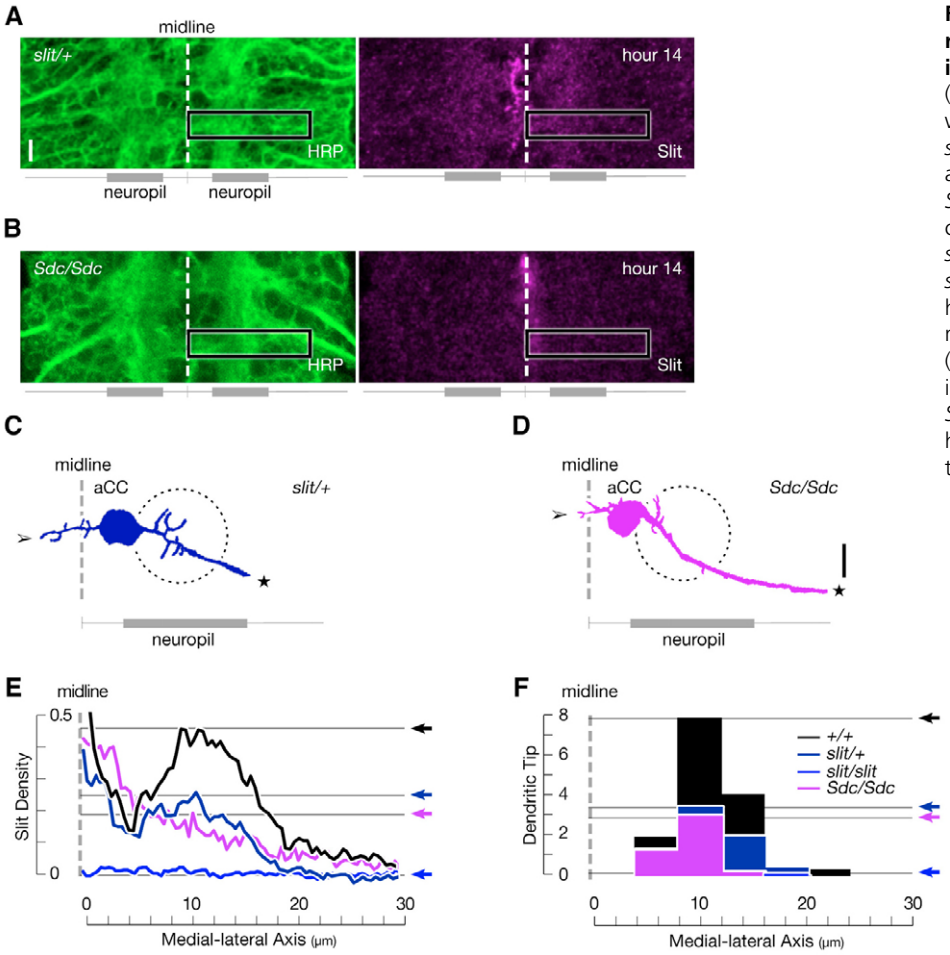

Fig. 9. Virtually wild-type neuropil but reduced Slit leads to small aCC dendrites in *slit/+* and *Sdc/Sdc* mutants. (**A**,**B**) Detergent-free immunocytochemistry with anti-HRP (green) and anti-Slit (purple) in $slit^2$/+ (A) and Sdc^{10608}/Sdc^{10608} (B) embryos at hour 14. (**C**,**D**) Tracing s of $slit^2$/+ (C) and Sdc^{10608}/Sdc^{10608} (D) aCCs at hour 17. (**E**) Slit concentration topography in +/+ (n=12), $slit^2$/+ (n=5), Sdc^{10608}/Sdc^{10608} (n=12) and $slit^2/slit^2$ (n=3) at hour 14. Arrows and horizontal lines indicate the maximum numbers of dendritic tips per bin. (**F**) Histogram of the number of dendritic tips in +/+ (n=14), $slit^2$/+ (n=12), Sdc^{10608}/Sdc^{10608} (n=14) and $slit^2/slit^2$ (n=9) aCCs at hour 17. Arrows and horizontal lines indicate the neuropilar peaks. Scale bar: 5 μm.

study develop a neuropil in the CNS. In all cases, the aCC forms collateral dendrites at the neuropil, but not anywhere else. However, no neuron that extends its axon or dendrite across the midline develops dendritic branches at the midline despite the fact that the midline is the sole source of Slit in the CNS (Furrer et al., 2003; Landgraf et al., 1997; Landgraf et al., 2003). Furthermore, we find that, unlike dissociated neurons in culture (Whitford et al., 2002), ectopic Slit presented outside of the CNS, at muscle-12, does not induce collateral dendrogenesis in aCC motoneurons (Fig. 10). What are the factors that spatially restrict the dendrogenic function of Slit-Robo signaling to the neuropil? It is possible that such factors are present at the neuropil itself, serving a permissive role. However, it is also conceivable that the active suppression of dendrogenesis occurs outside the neuropil, including at the CNS midline and outside the CNS. In addition to such extrinsic factors, each neuron could display intrinsic molecular biases towards a certain portion of its axon. If this were true, then one might anticipate finding mutations that cause reduced dendrites at the neuropil, as well as mutations that cause ectopic collateral dendrogenesis outside the neuropil. Recently, we have found several mutants that fit both of these categories (our unpublished results). Characterization of these mutations will not only help identify additional factors that impact dendrogenesis, but also offer insights into the general question of how spatiotemporal precision in dendrogenesis is regulated within the CNS.

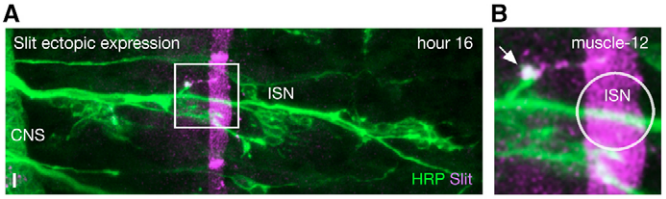

Fig. 10. Ectopic Slit is not sufficient to induce dendrogenesis outside the CNS. (**A**,**B**) Detergent-free immunocytochemistry with anti-HRP (green) and anti-Slit (purple) in embryo with Slit overexpression in muscle-12 ($GAL4^{M12}/UAS\text{-}slit^{WT}$) at hour 16. Box in A indicates the region shown in B. Even when faced with ectopic Slit, the aCC and other axons in the ISN do not produce ectopic collateral processes (circle). However, the RP5 axon fails to innervate its target, muscle-12 (arrow). Muscle-12 extends Slit-positive myopodia to contact the RP5 axon. Scale bar: 5 μm.

Slit and Robo as architects of the CNS

In the developing *Drosophila* CNS, the initial Slit topography before hour 14 is relatively simple, with a single peak at the midline (Fig. 5). There, Slit-Robo signaling repels axonal growth cones from the midline (Brose et al., 1999; Erskine et al., 2000; Hao et al., 2001; Kidd et al., 1999) and coordinates positioning of longitudinal fascicles (Rajagopalan et al., 2000; Simpson et al., 2000). As long as the midline peak persists, it continues to repel dendritic growth cones (Furrer et al., 2003). However, at the emerging neuropil, the concentration of extracellular Slit also rises steadily, creating a second Slit-enriched region within the developing CNS. Here, Slit-Robo signaling has an additional role as a promoter for dendrogenesis. Thus, the same Slit-Robo signaling that repels

growth cones from the midline, also produces dendrites at the neuropil, thereby sculpting the neural architecture at multiple stages. How various molecules that are known to impact dendritic morphology (Gao and Bogert, 2003; Grueber and Jan, 2004) may be linked to Slit-Robo signaling remains an open question. Future study is needed to address how Slit and its receptor Robo collaborate with diverse signaling partners at multiple steps of neural development, to serve as the 'architects' of the developing CNS.

We thank members of the Chiba laboratory for comments on the manuscript. This work was supported by grants from NIH/NINDS and NIH/NIMH (A.C.).

References

Brankatschk, M. and Dickson, B. J. (2006). Netrins guide Drosophila commissural axons at short range. *Nat. Neurosci.* **9**, 188-194.
Brose, K., Bland, K. S., Wang, K. H., Arnott, D., Henzel, W., Goodman, C. S., Tessier-Lavigne, M. and Kidd, T. (1999). Slit proteins bind Robo receptors and have an evolutionarily conserved role in repulsive axon guidance. *Cell* **96**, 795-806.
Erskine, L., Williams, S. E., Brose, K., Kidd, T., Rachel, R. A., Goodman, C. S., Tessier-Lavigne, M. and Mason, C. A. (2000). Retinal ganglion cell axon guidance in the mouse optic chiasm: expression and function of robos and slits. *J. Neurosci.* **20**, 4975-4982.
Fujioka, M., Lear, B. C., Landgraf, M., Yusibova, G. L., Zhou, J., Riley, K. M., Patel, N. H. and Jaynes, J. B. (2003). Even-skipped, acting as a repressor, regulates axonal projections in *Drosophila*. *Development* **130**, 5385-5400.
Furrer, M. P., Kim, S., Wolf, B. and Chiba, A. (2003). Robo and Frazzled/DCC mediate dendritic guidance at the CNS midline. *Nat. Neurosci.* **6**, 223-230.
Gao, F. B. and Bogert, B. A. (2003). Genetic control of dendritic morphogenesis in *Drosophila*. *Trends Neurosci.* **26**, 262-268.
Godenschwege, T. A., Simpson, J. H., Shan, X., Bashaw, G. J., Goodman, C. S. and Murphey, R. K. (2002). Ectopic expression in the giant fiber system of *Drosophila* reveals distinct roles for roundabout (Robo), Robo2, and Robo3 in dendritic guidance and synaptic connectivity. *J. Neurosci.* **22**, 3117-3129.
Goodhill, G. J. (2003). A theoretical model of axon guidance by the Robo code. *Neural Comput.* **15**, 549-564.
Grueber, W. B. and Jan, Y. N. (2004). Dendritic development: lessons from *Drosophila* and related branches. *Curr. Opin. Neurobiol.* **14**, 74-82.
Hao, J. C., Yu, T. W., Fujisawa, K., Culotti, J. G., Gengyo-Ando, K., Mitani, S., Moulder, G., Barstead, R., Tessier-Lavigne, M. and Bargmann, C. I. (2001). *C. elegans* slit acts in midline, dorsal-ventral, and anterior-posterior guidance via the SAX-3/Robo receptor. *Neuron* **32**, 25-38.
Hiramoto, M., Hiromi, Y., Giniger, E. and Hotta, Y. (2000). The *Drosophila* Netrin receptor Frazzled guides axons by controlling Netrin distribution. *Nature* **406**, 886-889.
Howitt, J. A., Clout, N. J. and Hohenester, E. (2004). Binding site for Robo receptors revealed by dissection of the leucine-rich repeat region of Slit. *EMBO J.* **23**, 4406-4412.
Jan, L. Y. and Jan, Y. N. (1982). Antibodies to horseradish peroxidase as specific neuronal markers in *Drosophila* and in grasshopper embryos. *Proc. Natl. Acad. Sci. USA* **79**, 2700-2704.
Johnson, K. G., Ghose, A., Epstein, E., Lincecum, J., O'Connor, M. B. and Van Vactor, D. (2004). Axonal heparan sulfate proteoglycans regulate the distribution and efficiency of the repellent slit during midline axon guidance. *Curr. Biol.* **14**, 499-504.
Kidd, T., Brose, K., Mitchell, K. J., Fetter, R. D., Tessier-Lavigne, M., Goodman, C. S. and Tear, G. (1998). Roundabout controls axon crossing of the CNS midline and defines a novel subfamily of evolutionarily conserved guidance receptors. *Cell* **92**, 205-215.
Kidd, T., Bland, K. S. and Goodman, C. S. (1999). Slit is the midline repellent for the Robo receptor in *Drosophila*. *Cell* **96**, 785-794.
Kim, S. and Chiba, A. (2004). Dendritic guidance. *Trends Neurosci.* **27**, 194-202.
Kramer, S. G., Kidd, T., Simpson, J. H. and Goodman, C. S. (2001). Switching repulsion to attraction: changing responses to slit during transition in mesoderm migration. *Science* **292**, 737-740.
Landgraf, M., Bossing, T., Technau, G. M. and Bate, M. (1997). The origin, location, and projections of the embryonic abdominal motoneurons of *Drosophila*. *J. Neurosci.* **17**, 9642-9655.
Landgraf, M., Jeffrey, V., Fujioka, M., Jaynes, J. B. and Bate, M. (2003). Embryonic origins of a motor system: motor dendrites form a myotopic map in *Drosophila*. *PLoS. Biol.* **1**, E41.
Li, H. S., Chen, J. H., Wu, W., Fagaly, T., Zhou, L., Yuan, W., Dupuis, S., Jiang, Z. H., Nash, W., Gick, C. et al. (1999). Vertebrate slit, a secreted ligand for the transmembrane protein roundabout, is a repellent for olfactory bulb axons. *Cell* **96**, 807-818.
Liu, Z., Patel, K., Schmidt, H., Andrews, W., Pini, A. and Sundaresan, V. (2004). Extracellular Ig domains 1 and 2 of Robo are important for ligand (Slit) binding. *Mol. Cell. Neurosci.* **26**, 232-240.
Miyashita, T., Yeo, S. Y., Hirate, Y., Segawa, H., Wada, H., Little, M. H., Yamada, T., Takahashi, N. and Okamoto, H. (2004). PlexinA4 is necessary as a downstream target of Islet2 to mediate Slit signaling for promotion of sensory axon branching. *Development* **131**, 3705-3715.
Ozdinler, P. H. and Erzurumlu, R. S. (2002). Slit2, a branching-arborization factor for sensory axons in the Mammalian CNS. *J. Neurosci.* **22**, 4540-4549.
Rajagopalan, S., Vivancos, V., Nicolas, E. and Dickson, B. J. (2000). Selecting a longitudinal pathway: Robo receptors specify the lateral position of axons in the *Drosophila* CNS. *Cell* **103**, 1033-1045.
Rothberg, J. M., Hartley, D. A., Walther, Z. and Artavanis-Tsakonas, S. (1988). slit: an EGF-homologous locus of D. melanogaster involved in the development of the embryonic central nervous system. *Cell* **55**, 1047-1059.
Rothberg, J. M., Jacobs, J. R., Goodman, C. S. and Artavanis-Tsakonas, S. (1990). slit: an extracellular protein necessary for development of midline glia and commissural axon pathways contains both EGF and LRR domains. *Genes Dev.* **4**, 2169-2187.
Simpson, J. H., Bland, K. S., Fetter, R. D. and Goodman, C. S. (2000). Short-range and long-range guidance by Slit and its Robo receptors: a combinatorial code of Robo receptors controls lateral position. *Cell* **103**, 1019-1032.
Sonnenfeld, M. J. and Jacobs, J. R. (1994). Mesectodermal cell fate analysis in Drosophila midline mutants. *Mech. Dev.* **46**, 3-13.
Steigemann, P., Molitor, A., Fellert, S., Jackle, H. and Vorbruggen, G. (2004). Heparan sulfate proteoglycan syndecan promotes axonal and myotube guidance by slit/robo signaling. *Curr. Biol.* **14**, 225-230.
Tabata, T. (2001). Genetics of morphogen gradients. *Nat. Rev. Genet.* **2**, 620-630.
Tayler, T. D., Robichaux, M. B. and Garrity, P. A. (2004). Compartmentalization of visual centers in the Drosophila brain requires Slit and Robo proteins. *Development* **131**, 5935-5945.
Tessier-Lavigne, M., Placzek, M., Lumsden, A. G., Dodd, J. and Jessell, T. M. (1988). Chemotropic guidance of developing axons in the mammalian central nervous system. *Nature* **336**, 775-778.
Vasenkova, I., Luginbuhl, D. and Chiba, A. (2006). Gliopodia extend the range of direct glia-neuron communication during the CNS development in *Drosophila*. *Mol. Cell. Biol.* **31**, 123-131.
Wang, K. H., Brose, K., Arnott, D., Kidd, T., Goodman, C. S., Henzel, W. and Tessier-Lavigne, M. (1999). Biochemical purification of a mammalian slit protein as a positive regulator of sensory axon elongation and branching. *Cell* **96**, 771-784.
Ward, M. E., Jiang, H. and Rao, Y. (2005). Regulated formation and selection of neuronal processes underlie directional guidance of neuronal migration. *Mol. Cell. Neurosci.* **30**, 378-387.
Westerfield, M., McMurray, J. V. and Eisen, J. S. (1986). Identified motoneurons and their innervation of axial muscles in the zebrafish. *J. Neurosci.* **6**, 2267-2277.
Whitford, K. L., Marillat, V., Stein, E., Goodman, C. S., Tessier-Lavigne, M., Chedotal, A. and Ghosh, A. (2002). Regulation of cortical dendrite development by Slit-Robo interactions. *Neuron* **33**, 47-61.
Wolf, B. D. and Chiba, A. (2000). Axon pathfinding proceeds normally despite disrupted growth cone decisions at CNS midline. *Development* **127**, 2001-2009.
Yeo, S. Y., Little, M. H., Yamada, T., Miyashita, T., Halloran, M. C., Kuwada, J. Y., Huh, T. L. and Okamoto, H. (2001). Overexpression of a slit homologue impairs convergent extension of the mesoderm and causes cyclopia in embryonic zebrafish. *Dev. Biol.* **230**, 1-17.
Yuan, W., Zhou, L., Chen, J. H., Wu, J. Y., Rao, Y. and Ornitz, D. M. (1999). The mouse SLIT family: secreted ligands for ROBO expressed in patterns that suggest a role in morphogenesis and axon guidance. *Dev. Biol.* **212**, 290-306.
Zou, Y., Stoeckli, E., Chen, H. and Tessier-Lavigne, M. (2000). Squeezing axons out of the gray matter: a role for slit and semaphorin proteins from midline and ventral spinal cord. *Cell* **102**, 363-375.